Applied Energy **30** (1988) 99–111

Stratified Thermal Storage Tank Inlet Mixing Characterization

Y. H. Zurigat, A. J. Ghajar & P. M. Moretti

School of Mechanical and Aerospace Engineering, Oklahoma State University, Stillwater, Oklahoma 74078, USA

ABSTRACT

Predictions of thermocline development in thermocline thermal storage tanks can be made by accounting for turbulent mixing at the inlet region. A practical measure for quantifying this mixing is obtained by introducing an effective diffusivity factor in a one-dimensional flow model. Thus, a tool for characterization of turbulent mixing caused by different inlet configurations is now available. This should facilitate the selection of diffusers for achieving a high degree of stratification in thermocline thermal storage tanks.

NOTATION

c	Concentration (percent by weight).
c_p	Specific heat.
d	Hydraulic diameter of the inlet port.
Fo	Fourier number, $Fo = \alpha \Delta t/\Delta x^2$.
g	Acceleration due to gravity.
H	Effective height between tank inlet and outlet.
k	Thermal conductivity.
k_t	Eddy conductivity.
N_{sl}	Number of finite-difference grid point.
N_{slt}	Total number of grid points.
Q	Volumetric flow rate.
Re	Reynolds number, $Re = \rho V d/\mu$.
Ri	Richardson number, $Ri = \Delta\rho g H/\rho_m V^2$.

Applied Energy 0306-2619/88/$03·50 © 1988 Elsevier Applied Science Publishers Ltd, England. Printed in Great Britain

T Temperature.
t Time.
T^* Dimensionless temperature, $T^* = (T - T_{in})/(T_o - T_{in})$.
t^* Dimensionless time, $t^* = tV_m/H$.
V Mean velocity based on inlet port area.
V_m Mean vertical velocity in the tank.
x Vertical distance.
α Thermal diffusivity, $\alpha = \rho c_p/k$.
α^* Effective thermal diffusivity, $\alpha^* = \alpha + \varepsilon_H$.
ε_H Eddy diffusivity for heat, $\varepsilon_H = \rho c_p/k_t$.
ε_{eff} Effective diffusivity factor, $\varepsilon_{eff} = \alpha^*/\alpha$.
μ Dynamic viscosity.
ρ Density.
$\Delta\rho$ Density difference between the cold and hot fluids.
ΔT Temperature difference between the cold and hot fluids.

Subscripts
eff Effective.
fw Fresh water.
in Inlet.
m Mean value.
n At point n.
o Initial.
s Salt (sodium chloride).
sw Saline water.

Superscripts
$'$ At a future time step.
in Value at the inlet.

INTRODUCTION

Sensible thermal storage in water has been recognized as an effective tool in extending the use of solar heating through a larger part of the day. Conversely, chilled-water storage is used to reduce utility bills and capital investment in air-conditioning systems. Thus, thermal storage is an attractive option for both heating and cooling applications.

The efficiency of systems employing sensible thermal storage in water depends largely on maintaining the separation of the warmer and colder water in the tank throughout the operating cycle. It is important that the hot or chilled water being stored experiences minimum mixing during the process of charging and discharging. This is the key factor in maintaining the thermodynamic availability of the stored energy as well as ensuring high efficiencies of chillers or solar collectors in the system.[1,2] Multiple tanks are one obvious way of achieving separation, but are not the best choice with regard to simplicity, economic feasibility and space utilization. Other schemes have been designed and implemented,[3] i.e. a single tank with diaphragm mounted either horizontally or vertically, labyrinth tanks in which the water is forced to flow through a maze, and the single stratified tank in which use is made of the natural process of stratification that permits the hot water to float on top of the cold water.

The single stratified tank (SST) is the most attractive choice due to its simplicity and low cost. Moreover, the performance of the SST is comparable with the other types.[4] This type of thermal storage has been the subject of many investigations in the past, both analytical and experimental. The thermal performance of a stratified tank depends on the thermocline (being the region of the steepest temperature gradient in the stratified fluid body) thickness that can be maintained; this is a function of several factors, i.e. the rate of heat loss to the surroundings, buoyancy-driven motions in the fluid body, heat conduction along the walls and, most importantly, the flow near the inlet. The objective is to maintain the thermocline region as thin as possible. Therefore the problem of predicting thermocline development for a given inlet configuration is fundamental.

In previous studies[5,6] an analytical model was developed to track the thermocline in a stratified tank. An effective diffusivity factor, $\varepsilon_{\mathrm{eff}}$, was introduced in the model to account for the mixing processes in the fluid. When applying the model to the experimental data in the literature and to our own, it was found that this factor varies from a maximum at the inlet to a minimum of one at the outlet in a decreasing hyperbolic function where the inlet value is dependent on the inlet flow conditions.[6] This result shows explicitly that mixing near the inlet has primary influence on the shape of the thermocline. Thus, the effectiveness of the inlet design in diffusing high velocities is central to the avoidance of mixing. In this study turbulent mixing, represented by $\varepsilon_{\mathrm{eff}}$, at the inlet region of thermocline thermal storage tanks is investigated using flow simulation and experimental data.

EFFECTIVE DIFFUSIVITY FACTOR (EDF)

The numerical model in which the EDF was introduced is described in detail in Ref. 5. Therefore only a brief outline is given here as related to the EDF.

The one-dimensional energy equation governing the turbulent flow in stratified tanks is given by

$$\frac{\partial T}{\partial t} + V\frac{\partial T}{\partial x} = (\alpha + \alpha_{\mathrm{H}})\frac{\partial^2 T}{\partial x^2} = \alpha^* \frac{\partial^2 T}{\partial x^2} \tag{1}$$

or by multiplying and dividing α^* by α

$$\frac{\partial T}{\partial t} + V\frac{\partial T}{\partial x} = \alpha\varepsilon_{\text{eff}}\frac{\partial^2 T}{\partial x^2} \tag{2}$$

where $\varepsilon_{\text{eff}} = \alpha^*/\alpha$ is the effective diffusivity factor having the effect of magnifying the molecular thermal diffusivity for turbulence. Thus we have $\varepsilon_{\text{eff}} = 1$ for laminar flow and $\varepsilon_{\text{eff}} \gg 1$ for turbulent flow. In order to completely eliminate the numerical diffusion inherent in the first-order upwind differencing of the convection term, eqn (2) was split into two limiting cases, namely the pure convection case ($\alpha = 0$) and the conduction case ($V = 0$). Thus we have for the former case

$$\frac{\partial T}{\partial t} + V\frac{\partial T}{\partial x} = 0 \tag{3}$$

and for the latter case

$$\frac{\partial T}{\partial t} = \alpha\varepsilon_{\text{eff}}\frac{\partial^2 T}{\partial x^2} \tag{4}$$

The stability of the finite-difference solution of eqn (3) requires that

$$\frac{V\Delta t}{\Delta x} = 1{\cdot}0$$

for the constant flow rate, or

$$\frac{V\Delta t}{\Delta x} \leq 1{\cdot}0 \tag{5}$$

for the more general case of variable flow rate which was handled by the 'buffer tank' concept.[5] The implicit finite-difference representation of eqn (4) is given by

$$(-\varepsilon_{\text{eff}}Fo)T'_{n-1} + (1 + 2\varepsilon_{\text{eff}}Fo)T'_n + (-\varepsilon_{\text{eff}}Fo)T'_{n-1} = T_n \tag{6}$$

The system of eqn (6) is solved using tridiagonal matrix algorithm (TDMA) subject to the restriction given by eqn (5) and the appropriate initial and boundary conditions (see Ref. 5).

As stated earlier, the variation of ε_{eff} with height was found to be of hyperbolic form:

$$\varepsilon_{\text{eff}} = A/N_{\text{sl}} + B \tag{7}$$

where $A = (\varepsilon_{\text{eff}}^{\text{in}} - 1)/(1 - 1/N_{\text{slt}})$, $B = \varepsilon_{\text{eff}}^{\text{in}} - A$ and N_{sl} is the number of the computational grid point in increasing order from the inlet.

The total number of the finite-difference grid points, N_{slt}, is determined by

$$N_{\text{slt}} = H/(V_{\text{m}}\Delta t) \tag{8}$$

The value of ε_{eff} at the inlet, $\varepsilon_{\text{eff}}^{\text{in}}$, needs to be determined. However, some

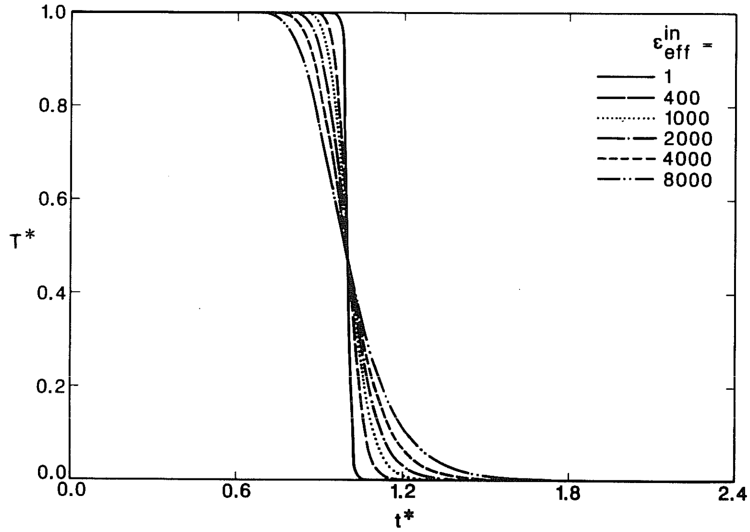

Fig. 1. Thermocline profiles for different values of ε_{eff}^{in}.

comments about its significance are in order. Figure 1 shows the model's predictions for the thermocline for different values of ε_{eff}^{in}. Note that perfect stratification occurs at ε_{eff}^{in} of one. As ε_{eff}^{in} increases, the model predicts a wider thermocline, i.e. more mixing. This shows that:

(1) the effective diffusivity factor introduced in this model may be used to quantify the turbulent effects in thermocline thermal storage tanks; and
(2) this factor, if correlated with the flow parameters, may serve as a tool to identify the best inlet configuration for high performance.

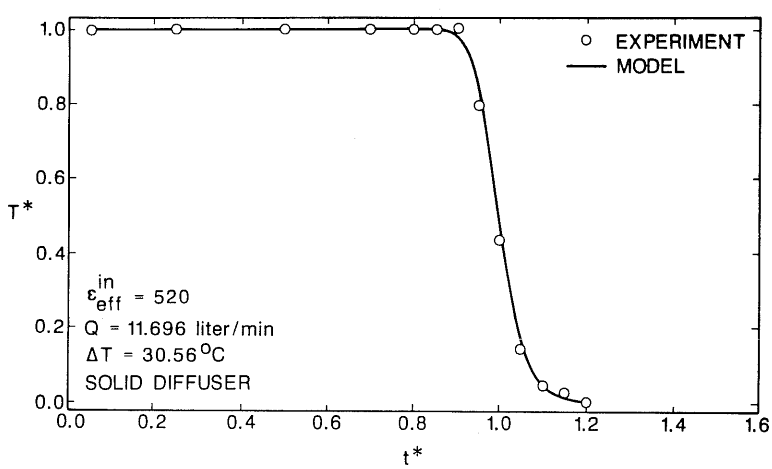

Fig. 2. Model fitted to the experiment for $\varepsilon_{eff}^{in} = 520$.

A typical comparison between the predictions and experimental results is shown in Fig. 2, where an inlet $\varepsilon_{\text{eff}}^{\text{in}}$ of 520 was specified based on the procedure that will be described in a later section. The objective of this study is to establish the relationship between $\varepsilon_{\text{eff}}^{\text{in}}$ and the flow parameters for a given inlet configuration.

EXPERIMENTS WITH FRESH–SALINE WATER SYSTEM

To investigate the behavior of the effective diffusivity factor introduced in the previous section, density-profile measurements were conducted using a fresh–saline water system with a plexiglas test tank of 0·2905 m diameter and 1·265 m height (see Fig. 3). This is particularly useful in obtaining a wide range of densities. Furthermore, the assumption of no-heat-loss adopted by the analytical model is satisfied and flow visualization of the thermocline development can be easily accomplished.

Using a fresh–saline water system, the desired temperature difference between the tank inlet and tank initial fluid temperatures is determined first and the corresponding density difference is then obtained from the density versus temperature curve for water at atmospheric pressure. Thus

$$\Delta\rho = |\rho(T_o) - \rho(T_{\text{in}})| \tag{9}$$

The density of the saline water needed to produce the temperature difference is then

$$\rho_{\text{sw}} = \rho_{\text{fw}} + \Delta\rho \tag{10}$$

The corresponding concentration of salt in fresh water is determined by

$$c = \left[\frac{\rho_{\text{fw}}}{\rho_{\text{sw}}} - 1\right] \Big/ \left[\frac{\rho_{\text{fw}}}{\rho_{\text{s}}} - 1\right] \tag{11}$$

Once the required concentration is found, the saline solution is prepared in the mixing tank (see Fig. 3) by adding the appropriate amount of sodium chloride as verified by a calibrated conductivity probe. The test procedure is to fill the test tank with fresh water and introduce saline water at the bottom of the tank from a constant head container (see Fig. 3). A conductivity probe placed at the centerline of the test tank at the level of the outlet port was used to measure the voltage which was reduced to concentration equivalents using the calibration curve. Then the saline water density, ρ_{sw}, is determined from eqn (11) rearranged as

$$\rho_{\text{sw}} = \frac{\rho_{\text{fw}}}{1 + c\left(\dfrac{\rho_{\text{fw}}}{\rho_{\text{s}}} - 1\right)} \tag{12}$$

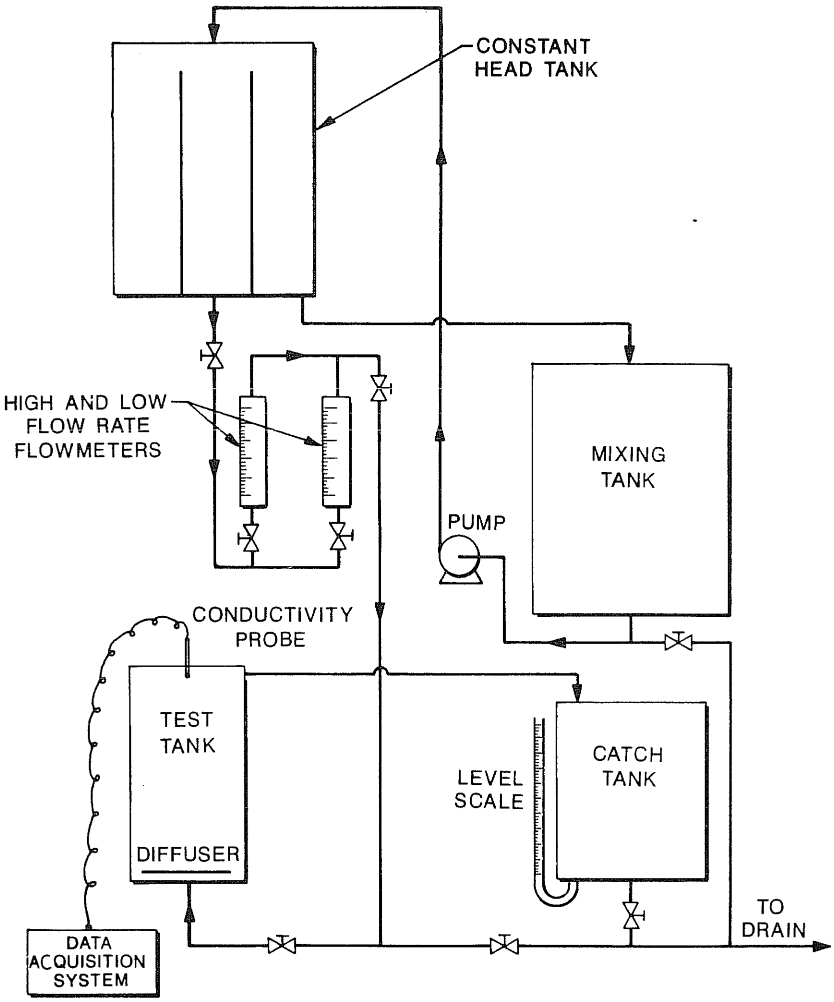

Fig. 3. Schematic of the experimental setup for fresh–saline water system.

At $c = 0$, $\rho_{sw} = \rho_{fw}$ and, upon conversion to temperature, $T_{sw} = T_{fw}$. For measured concentrations ($c > 0$; $\rho_{sw} > \rho_{fw}$), the resulting temperature corresponding to ρ_{sw} is much lower than that corresponding to ρ_{fw} and it could be in the negative region of temperatures when direct conversion of density to temperature is made. Therefore a shift in densities downward by $\Delta\rho$ is employed, where $\Delta\rho$ is given by eqn (9). Thus an effective density is defined as

$$\rho_{eff} = \rho_{sw} - \Delta\rho \tag{13}$$

The effective density is then converted into temperature equivalent.

The following example illustrates the above-mentioned procedure.

Suppose it is desired to run an experiment with $\Delta T = 8{\cdot}3°C$ with fresh water being at a temperature of 7·8°C, i.e. $T_{fw} = 7{\cdot}8°C$. What is the required initial saline water concentration, c_o, and what is the temperature equivalent of some measured concentration, c $(0 < c < c_o)$?

The density difference is determined from eqn (9) as

$$\Delta\rho = |\rho(7{\cdot}8) - \rho(16{\cdot}1)| = 2{\cdot}467\ \text{kg/m}^3$$

where $\rho(T)$ is calculated from the density–temperature relations for fresh water at atmospheric pressure.

The saline water density is then calculated by eqn (10):

$$\rho_{sw} = 1003{\cdot}05\ \text{kg/m}^3$$

and c_o from eqn (11) with $\rho_s = 2159{\cdot}3\ \text{kg/m}^3$ is

$$c_o = 0{\cdot}004\,58 \text{ (or } 0{\cdot}458\% \text{ by weight)}$$

For any $0 < c < c_o$, say $c = 0{\cdot}004$ (or 0·4%), the corresponding density is determined by eqn (12):

$$\rho_{sw} = 1002{\cdot}73\ \text{kg/m}^3$$

and the effective density from eqn (13) is

$$\rho_{eff} = 1000{\cdot}26\ \text{kg/m}^3$$

which corresponds to a fresh water temperature of 8·9°C.

Using the aforementioned procedure, outlet temperature versus time curves were obtained for each experiment. Three types of inlet having the same opening area (0·002 88 m²) were investigated (see Fig. 4). The diffusers were mounted 0·051 m from the bottom of the tank. For each inlet con-

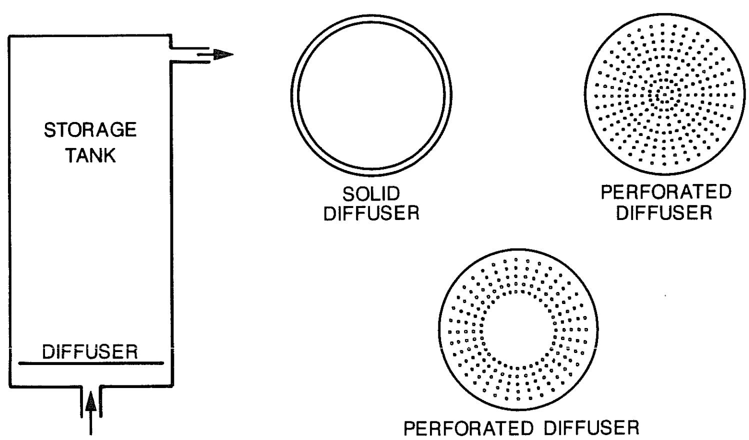

Fig. 4. Types of inlet configuration tested.

figuration, tests were carried out at different flow rates with three different concentrations each. The flow rates used were 3·596–12·188 liters/min with concentrations ranging from 0·46% to 2·0% salt (by weight). These concentrations correspond approximately to temperature differences of 8·33–33·3°C, respectively. The fresh water temperature varied from 7·8 to 11·1°C during the experiments. The concentration of saline water was determined with a conductivity probe by measuring the voltage at time intervals ranging from 1 min to 10 s. The 10-s sampling rate was used primarily in the thermocline region to facilitate adequate resolution. The voltage was converted to concentration using standard solution calibration data.

RESULTS AND DISCUSSION

As can be seen in Fig. 1, the thermocline shape varies with the inlet effective diffusivity factor, ε_{eff}^{in}. In order to obtain the values of ε_{eff}^{in} for different flow parameters and inlet conditions, the simulation program based on the model outlined is run with an initial guess that is incremented by the program. Comparison of the predicted thermocline for different values of ε_{eff}^{in} with the experimentally obtained thermocline establishes the best choice of ε_{eff}^{in}. Typical results of the calculated temperature profiles based on the best ε_{eff}^{in} are shown in Figs 2 and 5 with the corresponding ε_{eff}^{in} as indicated.

A plot of the best values of ε_{eff}^{in} versus flow rate for three different temperature differences, ΔT, is shown in Fig. 6. It can be seen that ε_{eff}^{in} increases with the flow rate and decreases with the increase in ΔT. This shows

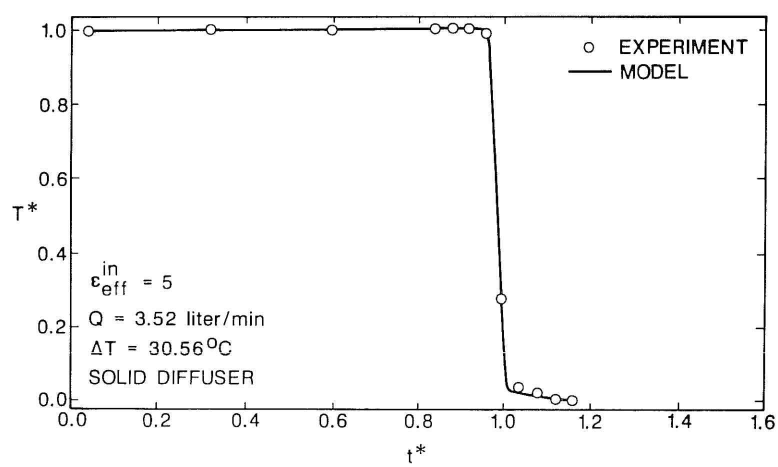

Fig. 5. Model fitted to the experiment with $\varepsilon_{eff}^{in} = 5$.

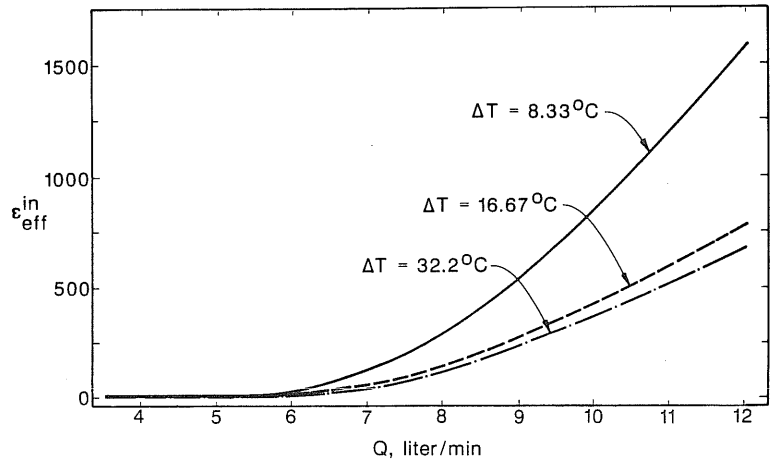

Fig. 6. Combined effect of flow parameters on ε_{eff}^{in}.

that the parameters affecting the rate of mixing at the inlet and the degree of stratification thereafter are the Reynolds and Richardson numbers. It can be observed that at low Reynolds numbers (i.e. low flow rates) ε_{eff}^{in} asymptotically approaches a minimum constant value of approximately 5. Note that at low flow rates ΔT has little effect on ε_{eff}^{in}. Thus, for any temperature difference, a minimum mixing effect results if the mean velocity in the tank is maintained below 0·001 524 m/sec (corresponding to 6 liters/min in Fig. 6). This is slightly higher than the value of 0·001 016 m/sec reported by Abdoly and Rapp.[7] However, the results presented here are based on measurements with a fresh–saline water system while those of Ref. 7 are based on hot–cold water system measurements.

In view of the above limits, it should be noted that the flow mean vertical velocity may not be a good indicator of the turbulence induced by the inlet geometry. Therefore, to maintain generality, it is desirable to express the above results in terms of dimensionless numbers. When the above results are expressed in terms of a Richardson number, a corresponding value of Ri of 5 was obtained. This value is higher than the reported value of unity recommended by Ref. 4 as the lower limit on the Richardson number for maintaining a high degree of stratification in chilled water storage. However, the recommended value of unity was in combination with additional requirements regarding the flow direction and the inlet diffuser design (see Ref. 4). In this study a Richardson number of 5 is recommended as the lower limit below which the layout of inlet diffusers starts to affect the degree of stratification attainable.

The experimental results showed little difference in thermocline shape for the types of diffusers investigated, especially at high temperature differences. The results for the lowest ΔT showed relatively the highest difference

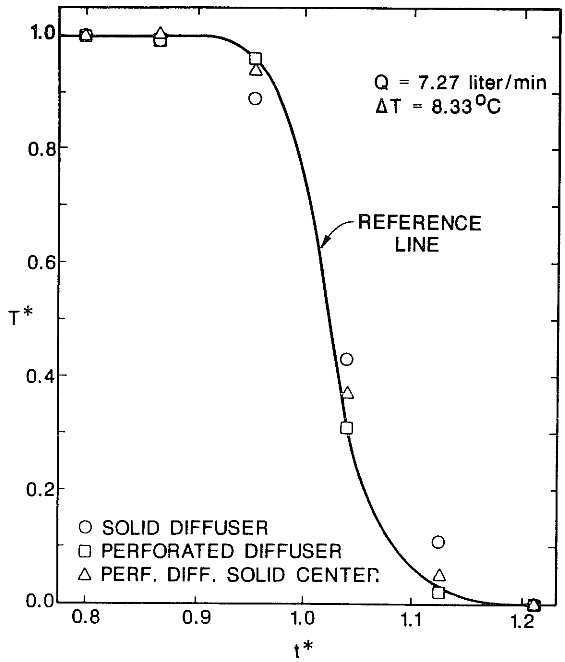

Fig. 7. Comparison of the performance of the inlet diffusers tested.

although small (see Fig. 7). In this range the perforated diffuser consistently had the best performance among the diffusers tested. The ratio of Reynolds to Richardson numbers seems to be the parameter governing the performance of the thermocline thermal storage tank. For higher values of *Re*/*Ri*, differences in performance of the inlet diffusers will occur. This is expected, because at low Richardson numbers or high Reynolds numbers (i.e. high *Re*/*Ri*) turbulent mixing at the inlet is dominant and the layout of inlet diffusers is important while at high Richardson numbers or low Reynolds numbers (i.e. low *Re*/*Ri*) high buoyancy forces inhibit mixing at the inlet region and different inlet configurations contribute less to the thermocline development.

Based on the above discussion, it can be stated that the effective diffusivity factor introduced in this study is a useful measure of mixing caused by the inlet design configurations. Therefore correlation of $\varepsilon_{\mathrm{eff}}^{\mathrm{in}}$ with the flow parameters and inlet configurations is desired. This can be done using experimental data. However, the experiments with a fresh–saline water system may be characterized as being qualitative in nature since the heat-mass transfer analogy is expected to be inexact. Therefore using experimental data from a hot–cold water system would be more fruitful in obtaining the desired correlations, a matter to be pursued further.

SUMMARY AND CONCLUSIONS

The success of large energy systems' simulation programs depends largely on the availability of efficient simulation subprograms for the systems' components. In this study predictions of thermocline development in a thermocline thermal storage tank were investigated. It was shown that these predictions can be made by accounting for turbulent mixing at the inlet region which was done by introducing an effective diffusivity factor, ε_{eff}. It was found that at low values of Re/Ri different inlet configurations perform well. Accordingly the inlet effective diffusivity factor, ε_{eff}^{in}, approaches a minimum constant value of 5, which indicates the role of buoyancy in suppressing turbulent mixing at the inlet of the storage tank. This corresponds to a limiting maximum mean velocity of 0·001 524 m/sec. A corresponding Richardson number of 5 was found to be the lower limit below which the diffuser design and layout starts to be a determining factor in thermocline thermal storage tank performance.

The effective diffusivity factor introduced in this study was shown to serve as a practical measure for quantification of mixing effects introduced by different inlet configurations. Thus a tool for characterization of inlet diffusers is now available. This should aid in obtaining diffuser information to facilitate the selection of diffusers for achieving high performance in thermocline thermal storage tanks.

ACKNOWLEDGEMENTS

This work was supported by the University Center for Energy Research (UCER) at Oklahoma State University. The assistance of Mr G. M. Hanna with the experiments and the helpful suggestions of Dr Y. Sharaf-Eldeen are gratefully acknowledged.

REFERENCES

1. M. K. Sharp and R. I. Loehrke, Stratified versus well-mixed sensible heat storage in a solar space heating application, ASME Paper 78-HT-49, Second AIAA–ASME Thermophysics and Heat Transfer Conference, Palo Alto, California, May 1978.
2. K. N. Shukla, Thermal energy storage for solar power generation: state of the art, *Heat Transfer Engng*, **3**(2) (1981), pp. 62–72.
3. R. T. Tamblyn, Thermal storage resisting temperature blending, *ASHRAE J.* (Jan. 1980), pp. 65–70.

4. M. W. Wilden and C. R. Truman, Evaluation study of stratified chilled-water storage technique, EPRI Report EPRI EM-4352, December 1985.
5. F. J. Oppel, A. J. Ghajar and P. M. Moretti, Computer simulation of stratified heat storage, *Applied Energy*, **23** (1986), pp. 205–24.
6. F. J. Oppel, A. J. Ghajar and P. M. Moretti, A numerical and experimental study of stratified thermal storage, *ASHRAE Trans.*, **92**(2) (1986), pp. 293–309.
7. M. A. Abdoly and D. Rapp, Theoretical and experimental study of stratified thermocline storage of hot water, *Energy Convers. Mgmt*, **22** (1982), pp. 275–85.